Pramāṇa, Vol. 18, No. 1, January 1982, pp. 99–112. © Printed in India.

# Neutral particle modelling assumptions: Theory and experiment

R JONES
Physics Department, National University of Singapore, Singapore 1025

MS received 13 July 1981; revised 31 October 1981

**Abstract.** The neutral particle recycling models that have been used to date in numerical plasma confinement simulations are by no means equivalent but may lead, instead, to divergent results. As a consequence of this confinement studies based on individual neutral assumptions must be received with a healthy degree of scepticism.

We go on to compare experimental observations of the time development of plasma density, temperature, and neutral pressure made in an electrostatic surface trap with numerical plasma simulations incorporating a number of alternative neutral models.

**Keywords.** Neutral particle models; plasma simulations; plasma confinement.

## 1. Introduction

Computational models have become an important tool in the detailed analysis of plasma confinement systems. Such models are used in scoping studies for projected thermonuclear reactors as well as for interpreting the results of present day plasma physics experiments. In order to complete the set of particle and energy balance equations in such computer codes it is necessary to include a dynamical description of the behaviour of the neutral refuelling gas. The sensitivity of the plasma physics results, to an alteration in the neutral model has, unfortunately, remained a largely unresolved question.

The various neutral particle assumptions have generally been used wholly independent of one another and their impact on the final results of simulations has generally gone unnoticed. In some (very few) instances where more than one neutral model was considered, the impact on the final computation has (sometimes) proved significant (Jaeger and Hedrick 1979; Jaeger *et al* 1979). Unfortunately, no systematic comparisons have been published up to this time. In the present paper we have sought to determine the impact of (a variety of) neutral particle models on a single common plasma simulation code. We have restricted our attention in this work to a global (zero dimensional) plasma model. Although it is anticipated that spatially resolved simulations will be even more sensitive to neutral modelling assumptions, a wide range of variables becomes necessary and detailed comparisons are difficult (voluminous).

## 2. The global plasma confinement model

Each of the neutral models is exercised in conjunction with a common set of plasma

particle and energy balance equations. The global averaged plasma density, $n_e$, (in $10^9$ cm$^{-3}$) is obtained as a function of time, by integrating

$$\dot{n}_e = \dot{n}_e|_{\text{ionize}} - \dot{n}_e|_{\text{diffuse}} - \dot{n}_e|_{\text{end loss}}, \tag{1}$$

where the gas is ionized at a rate given by (Drawin 1967):

$$\dot{n}_e|_{\text{ionize}} = \frac{371\, n_e\, n_n \exp(-15{\cdot}6/T_e)}{\left(\frac{15{\cdot}6 + T_e}{T_e}\right)(T_e)^{1/2}} \times \left[\frac{T_e}{15{\cdot}6 + 20\, T_e} + \ln\left(\frac{19{\cdot}5 + 1{\cdot}25\, T_e}{15{\cdot}6}\right)\right]. \tag{2}$$

Cross-field diffusion loss is given by (Kovrizhnykh 1969)

$$\dot{n}_e|_{\text{diffuse}} = \frac{\frac{1}{8} n_e^2}{B^2 R^2 T_e^{1/2}} + \frac{n_e\, n_n\, T_e}{B^2 R^2} 10^{-3}, \tag{3}$$

and adjustment of the parameters in (3) permits the modelling of the usual pseudo-classical wave induced 'anomalous' transport (Artsimovich 1972; Jones 1980a). $n_n$ is the globally averaged neutral density (in $10^9$ cm$^{-3}$), $B$ is the magnetic confining field (in kiloGauss), $R$ is the plasma radius (in cm), and $T_e$ is the electron temperature (in eV).

Particle end loss along open field lines (if any) is given by Jones (1979) as

$$\dot{n}_e|_{\text{end loss}} = \frac{2 n_e\, A\, (T_e + T_i)^{1/2}}{V} \times 10^5, \tag{4}$$

where $T_i$ is the ion plasma temperature (global average, in eV), $A$ is the loss area (in cm$^2$), and $V$ is the plasma volume (in cm$^3$).

The spatial average electron temperature, at each time step, is found by integrating

$$\dot{T}_e = \frac{1}{n_e}\left(\tfrac{2}{3}\dot{U}_e - T_e\, \dot{n}_e\right), \tag{5}$$

where the electron power density is just

$$\dot{U}_e = \dot{U}_e|_{\text{DT}} + \dot{U}_e|_{\text{in}} - \dot{U}_e|_{\text{ionize}} - \dot{U}_e|_{\text{brem}} - \dot{U}_e|_{\text{ions}} - \dot{U}_e|_{\text{diffuse}} - \dot{U}_e|_{\text{end loss}} - \dot{U}_e|_{\text{impurity}}. \tag{6}$$

The heating power input is

$$\dot{U}_e|_{\text{in}} = 2 \times 10^9 \frac{P}{V}, \tag{7}$$

where $P$ is expressed in watts. Fusion alpha particle heating can be included and enters through

$$\dot{U}_e|_{\mathrm{DT}} = \tfrac{1}{4} n_e^2 \langle \sigma v \rangle_{\mathrm{DT}} E_F, \tag{8}$$

where $E_F$ is the fusion energy release (3·52 MeV for the DT alpha particle, the energetic neutron escapes the plasma and heats the blanket) and the rate coefficient is:

$$\begin{aligned}\langle \sigma v \rangle_{\mathrm{DT}} = {} & 2{\cdot}87\times 10^{-16} - 8{\cdot}78\times 10^{-20}\, T_i \\ & + 1{\cdot}02\times 10^{-23}\, T_i^2 - 3{\cdot}74\times 10^{-28}\, T_i^3 + 4{\cdot}93\times 10^{-33}\, T_i^4.\end{aligned} \tag{9}$$

We assume here that the alphas give up their energy to electrons (by classical or anomalous processes) on a time scale faster than the times of interest.

Impurity radiation loss can be modelled for an (equilibrium) iron contaminant (a pessimistic assumption):

$$\dot{U}_e|_{\mathrm{impurity}} = 2\times 10^{9}\, G\, n_e\, n_I, \tag{10}$$

where

$$\begin{aligned}G = {} & 3{\cdot}3\times 10^{-28}\, T^{1/2} \\ & + 1{\cdot}4\times 10^{-27}\times 1{\cdot}21\times \exp\left(-[0{\cdot}194\{13{\cdot}12\,(|\log(T/13{\cdot}0)|)^{1{\cdot}43}+1\}]^{0{\cdot}701}\right) \\ & + 1{\cdot}9\times 10^{-27}\times 2{\cdot}11\times \exp\left(-[0{\cdot}744\,\{17{\cdot}94\,(|\log(T/13{\cdot}0)|)^{2{\cdot}24}+1\}]^{0{\cdot}447}\right. \\ & \qquad \left.\times\,(1-\exp[-(T/6{\cdot}4)^{2{\cdot}3}])\right) \\ & + 5{\cdot}1\times 10^{-27}\times 2{\cdot}75\times \exp\left(-[1{\cdot}01\,\{114{\cdot}6\,(|\log(T/6{\cdot}0)|)^{2{\cdot}95}+1\}]^{0{\cdot}340}\right) \\ & + 6{\cdot}6\times 10^{-27}\times 3{\cdot}79\times \exp\left(-[1{\cdot}33\,\{23{\cdot}41\,(|\log(T/1{\cdot}4)|)^{2{\cdot}17}+1\}]^{0{\cdot}460}\right) \\ & + 4{\cdot}0\times 10^{-26}\times 14{\cdot}50\times \exp\left(-[2{\cdot}67\{60{\cdot}69(|\log(T/0{\cdot}45)|)^{3{\cdot}56}+1\}]^{0{\cdot}281}\right),\end{aligned} \tag{11}$$

and $T = T_e \times 10^{-3} \geqslant 0{\cdot}4$ with $n_I$ the iron density (in cm$^{-3}$).

Ionization losses are accounted for by

$$\dot{U}_e|_{\mathrm{ionize}} = \dot{n}_e\,(E_I + eV_p + 3/2\, T_e), \tag{12}$$

where $E_I$ is the gas ionization energy, $e$ is the electronic charge, and $V_p$ is the plasma potential. For most applications we can take

$$eV_p = T_e \ln\,[(m_i/m_e)^{1/2}], \tag{13}$$

where $m_i/m_e$ is the ion to electron mass ratio (for hydrogen).

The Bremsstrahlung power loss is included by

$$\dot{U}_e|_{\text{brem}} = 10^{-4}\, n_e^2\, T_e^{1/2}, \tag{14}$$

and electron-ion collisional power transfer gives

$$\dot{U}_e|_{\text{ions}} = \frac{2{\cdot}3\, n_e^2\,(T_e - T_i)}{T_e^{3/2}} \ln\left[\frac{5{\cdot}2\times 10^{11}\, T_e^3}{n_e\,(40+T_e)}\right]. \tag{15}$$

The cross-field diffusion loss is given by

$$\dot{U}_e|_{\text{diffuse}} = 2{\cdot}5\, T_e\, \dot{n}_e|_{\text{diffuse}}, \tag{16}$$

and the end loss power density is just

$$\dot{U}_e|_{\text{end loss}} = 2\, T_e\, \dot{n}_e|_{\text{end loss}}. \tag{17}$$

The global average ion temperature, $T_i$, is obtained, as a function of time, by integrating

$$\dot{T}_i = \frac{1}{n_e}\left(\tfrac{2}{3}\,\dot{U}_i - T_i\,\dot{n}_e\right). \tag{18}$$

(By plasma neutrality $n_e = n_i$, the ion plasma density.) The ion power density is given by

$$\dot{U}_i = \dot{U}_e|_{\text{ions}} - \dot{U}_i|_{\text{CX}} - \dot{U}_i|_{\text{diffuse}} - \dot{U}_i|_{\text{end loss}}, \tag{19}$$

where the charge exchange loss is

$$\dot{U}_i|_{\text{CX}} = 0{\cdot}0732\, n_e\, n_n\, (T)^{3/2}\,(1 + 0{\cdot}00585 T_i^{3/2}) \exp(-0{\cdot}0582 T_i^{1/2}), \tag{20}$$

and the cross-field diffusion loss is

$$\dot{U}_i|_{\text{diffuse}} = 2{\cdot}5\, T_i\, \dot{n}_e|_{\text{diffuse}}. \tag{21}$$

Any end loss is accounted for by

$$\dot{U}_i|_{\text{end loss}} = 2\, T_i\, \dot{n}_e|_{\text{end loss}}. \tag{22}$$

This code has been used previously in RF heating calculations (Jones 1980c) and the present study grew out of a desire to further refine and improve it.

## 3. The various neutral particle models

In order to close the set of global particle (neutral, as well as charged) and energy balance equations one must provide, in addition to equations (1)–(22), a model for the (possibly) time dependent globally averaged neutral particle density, $n_n$. A wide variety of such neutral models have been suggested, each derived from (and justified by) its own set of physical assumptions.

### 3.1 *Time independent neutral density*

Some researchers have assumed that either the neutral density itself or the neutral flux into the plasma is a time independent quantity. The former assumption is justified by experience in " table top " plasma research devices in which an equilibrium is observed between cold gas injection and vacuum pumping. (A slightly more sophisticated assumption, based on complete and instantaneous neutralization at the wall, fixes the total particle density, $n_e + n_n$, rather than $n_n$ alone.) The latter assumption is appropriate if wall recycling is slow compared to the plasma confinement time (Jaeger *et al* 1979). Isotope exchange experiments (Marmer 1978; Simonov *et al* 1961; MoCracken *et al* 1978; Cohen *et al* 1978) have supported this assumption by demonstrating that gas previously absorbed in the wall determined the plasma isotopic abundance almost independent of the external cold gas feed (for times which are limited but which far exceed confinement time scales).

### 3.2 *Particle flux balance*

The neutral and charged particle populations can be considered to be competing species (Roth 1967) in a (generalized) Volterra sense and we recall (Goel *et al* 1971) that a pair of Volterra equations will have corresponding equilibrium equations of the form

$$\bar{n}_i = \bar{\nu}_n / l_i g, \tag{23}$$

and

$$\bar{n}_n = \bar{\nu}_i / l_n g, \tag{24}$$

where $g$ is the neutral gas ionization rate, $\bar{\nu}_{i,n}$ are the average ion and neutral flow speeds, and $l_{i,n}$ are the average ion and neutral flow distances. Total$^{(\text{average})}$ particle flux balance results from combining (23) and (24) (Jones 1980b):

$$\bar{n}_n \bar{\nu}_n = \bar{n}_e \bar{\nu}_i, \tag{25}$$

where $\bar{n}_e = \bar{n}_i$. In most codes this balance has been enforced instantaneously (Jaeger and Hedrick 1979).

### 3.3 *Neutral reflux velocity assumptions*

Before one can perform any actual calculations it is necessary to determine the value of $\bar{\nu}_n$ for use in (25). The total neutral flux is likely to be composed of a population

fraction of " cold " (ambient wall temperature) neutrals and a population of energetic " reflected " neutrals (Jones 1978a) whose energy will scale in proportion to the plasma temperature (rigorously, the temperature near the boundary if we were considering a one-dimensional code).

$$\bar{v}_n = \alpha \bar{v}_i + (1 - \alpha)\, v_{\text{th}}, \tag{26}$$

where $v_{\text{th}}$ is the thermal neutral speed (at the wall temperature).

### 3.4 *Wall reflection model*

If the reflected neutrals are assumed to dominate then (25) and (26) reduce to an equation of the form

$$n_e/n_n = \text{constant}. \tag{27}$$

### 3.5 *Constant density product model*

McBride and Sultan (1978) have suggested the zero-dimensional model equation

$$n_e\, n_n = \text{constant}, \tag{28}$$

as an accurate fit to the more detailed neutral transport studies of Berry *et al* (1974). No physical justification has been provided.

Numerical correction factors have sometimes been incorporated (into various of the foregoing models) in order to take some account of radial parametric dependences (*e.g.* finite neutral penetration and transit time effects of neutrals transversing the plasma radius, Sprott and Strait 1976). For our present study we chose to restrict attention to the lowest order differences between the various modelling assumptions and concern ourselves with a strictly zero-dimensional simulation. (If differences appear in 0-D they are likely to be even more pronounced in spatially resolved models.) Admixtures of the various models is also a possibility.

## 4. Computational results

In figures 1–3 we display the time development of the plasma parameters $T_e$, $n_e$, and $T_i$ for the various neutral models described in §3. The common set of initial conditions chosen for this example was:

$$T_e(0) = 5 \text{ eV}, \quad T_i(0) \cong 0 \text{ eV},$$

$$n_e(0) = 10^8 \text{ cm}^{-3}, \quad n_n(0) = 10^{10} \text{ cm}^{-3},$$

$$B = 10 \text{ kG}, \quad R = 10 \text{ cm}, \quad P/v = 5m \text{ Watt/cm}^3.$$

P is assumed constant in time. (For an alternative model, specialized to RF heating see Sprott and Strait 1976).

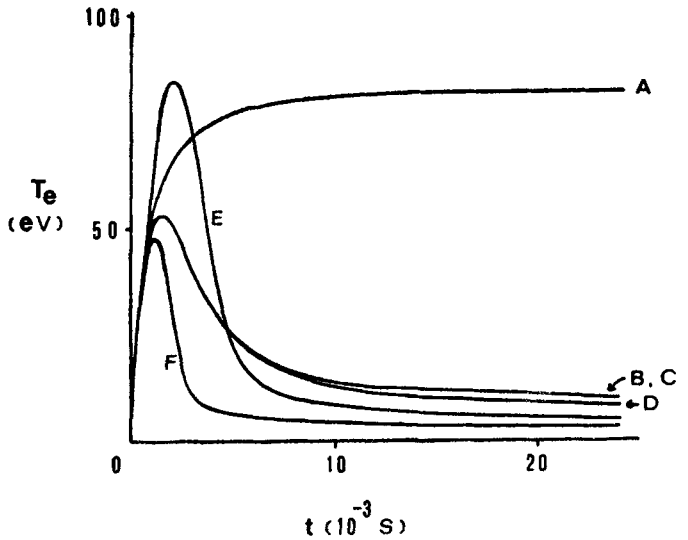


**Figure 1.** Electron temperatures *versus* time for various neutral models: A. $n_e \times n_n = C$, B. $n_e + n_n = C$, C. Wisconsin model (see Sprott and Strait 1976), D. $n_n = C$, E. Volterra model ($n_e/n_n = C/\sqrt{T_e}$), F. $n_e/n_n = C$.

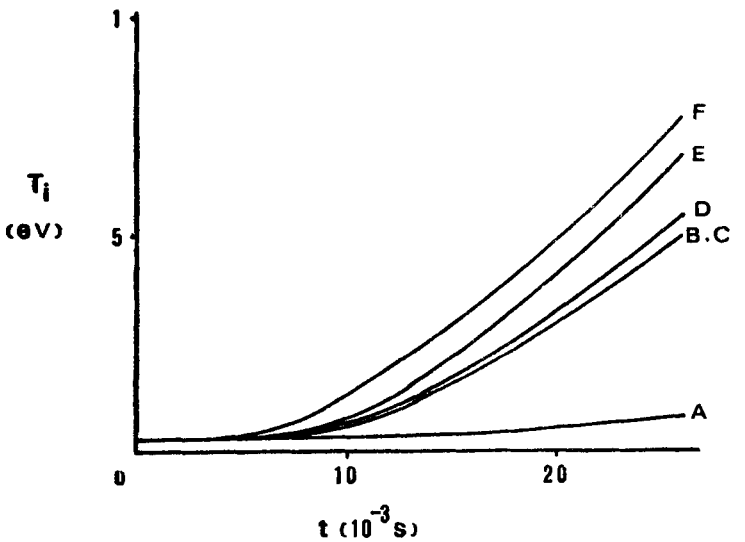


**Figure 2.** Ion temperature *versus* time for various neutral models.

The corresponding development of the neutral gas density is given in figure 4 and the parameters chosen are appropriate to small scale " table top " plasma research devices (Jones 1980b) having rather poorly ionized plasmas. It should be apparent from this example that the detailed parametric variations depend strongly on the neutral modelling assumptions: the higher electron temperatures corresponding to the lower neutral pressures (as might be expected, Jones 1979) while the higher ion temperatures and plasma densities occur for high neutral pressure (as can be anticipated from the functional forms of (2) and (15) as well as the neutral model

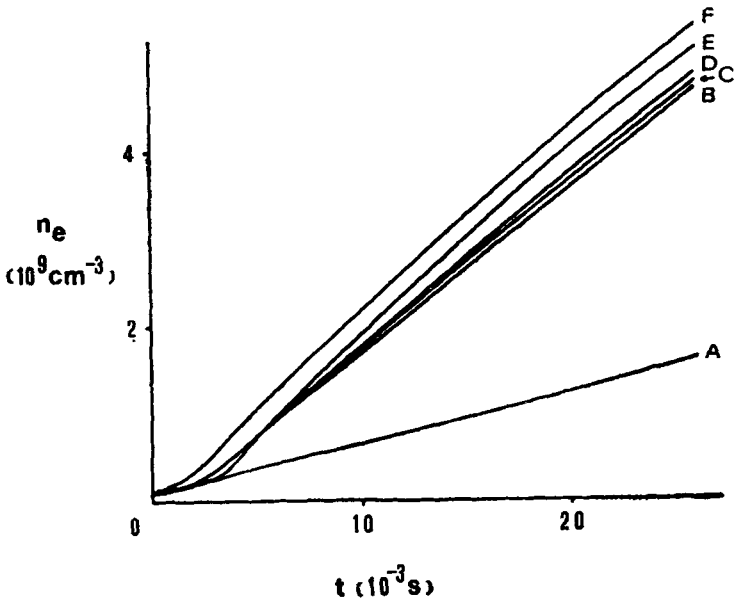


**Figure 3.** Plasma density *versus* time for various neutral models.

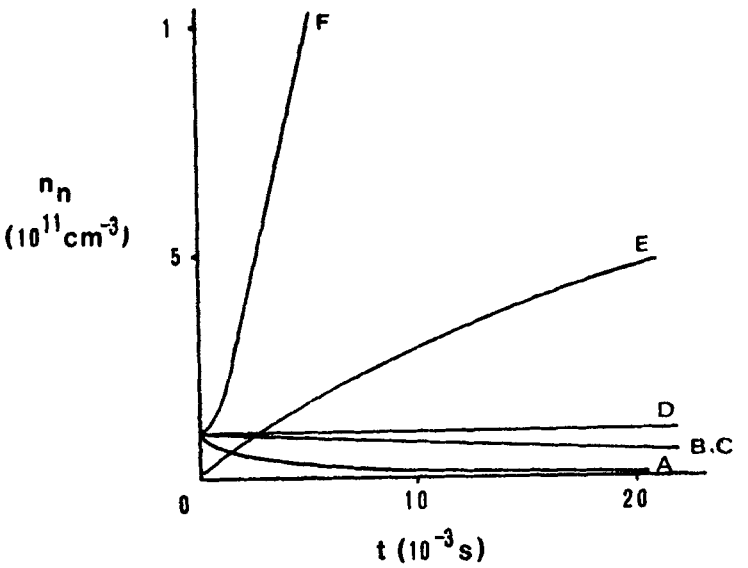


**Figure 4.** Neutral gas density *versus* time for various neutral models.

equations themselves). Such results can, in principle, be compared with limited experimental data taken in Levitron and Octopole type fusion devices. Experimental data obtained in the Wisconsin Octopole was taken expressly for this purpose (Sprott and Strait 1976) but, unfortnately, is limited to ion saturation current measurements.

$$J_i(t) = e n_e(t) \left( \frac{T_e(t)}{m_i} \right)^{1/2}. \tag{29}$$

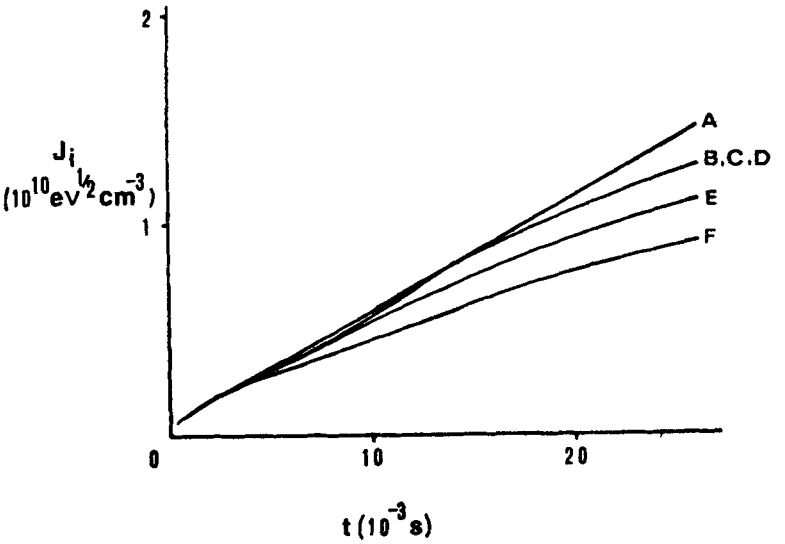


Figure 5. Ion saturation current density *versus* time for various neutral models.

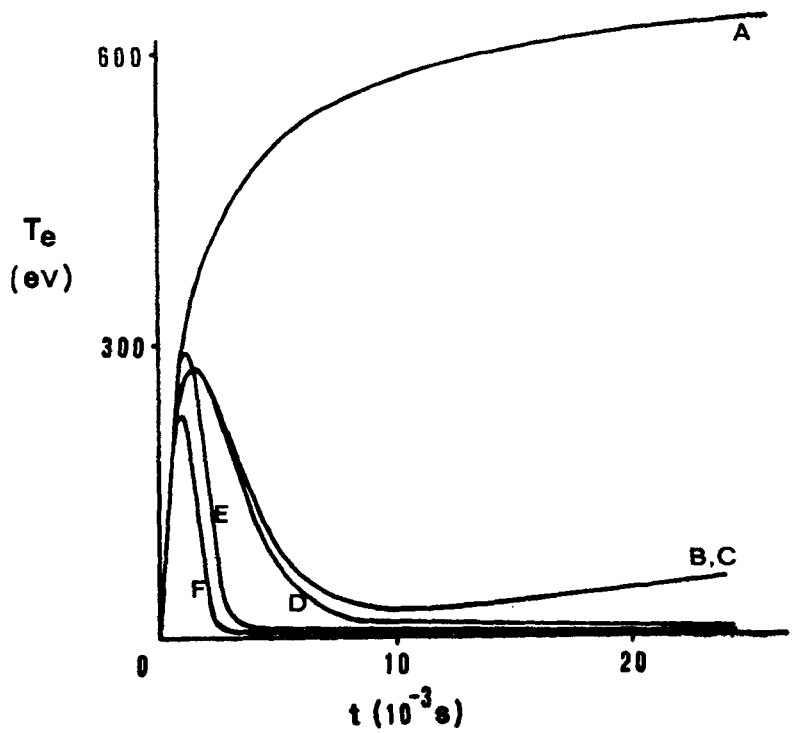


Figure 6. Electron temperature *versus* time for various neutral models.

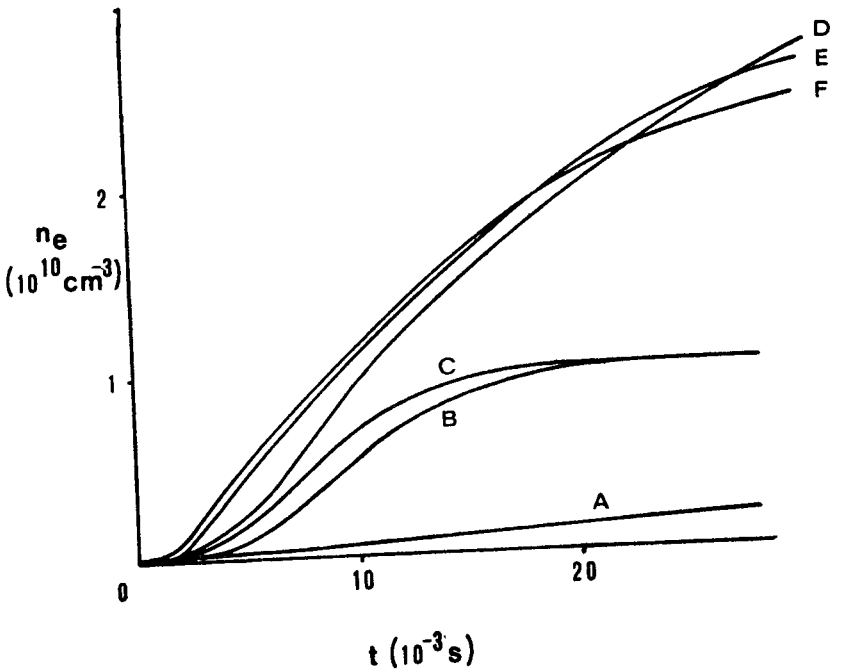


Figure 7. Plasma density *versus* time for various neutral models.

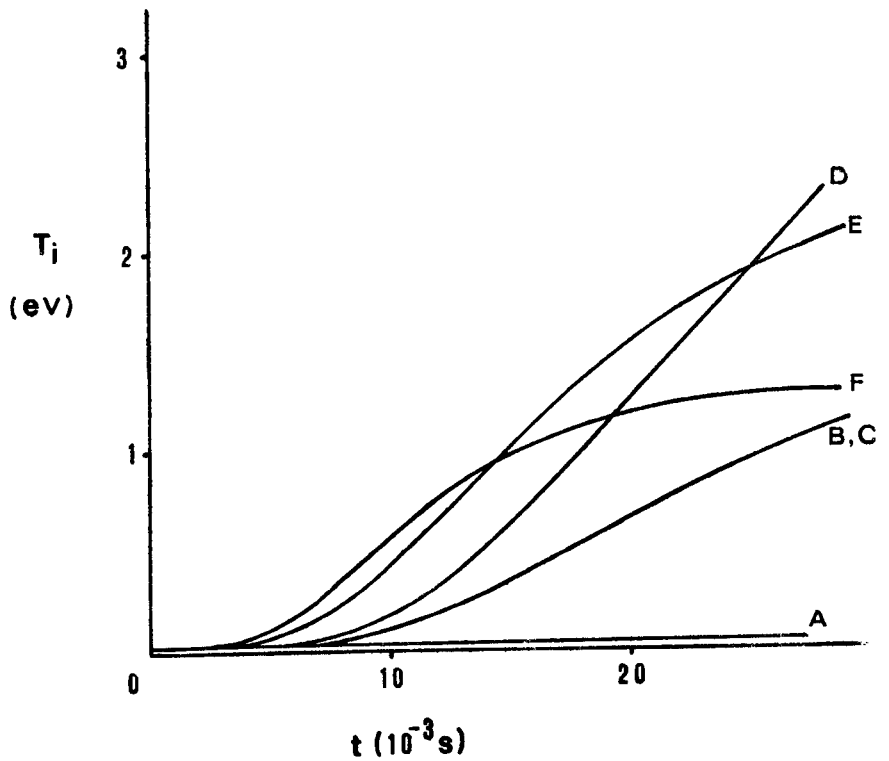


Figure 8. Ion temperature *versus* time for various neutral models.

Ion saturation current (figure 5) averages over the parametric deviations seen in figures 1–3 ($T_e$ and $n_e$ varying with $n_n$ in the opposite way) and it is not possible to distinguish between the various neutral models on this crude basis.

In figures 6–9 we display the time development of plasma parameters appropriate to a higher energy discharge. $(P/v) = 30$ m Watt/cm$^3$). Again we see significant differences, qualitatively similar to figures 1-4, and which are attributable to the different neutral assumptions imposed.

## 5. Experimental study

After noting the significance of the neutral modelling equation we decided to proceed to an experimental investigation. It is possible that different experimental devices might follow different neutral scaling laws and so we elected to employ plasma parameters which are not too different from those found near the boundary of present day and near term fusion experiments.

The experiments were performed as a part of the applications technology experiment (ATX) in the " U-1 " (Jones 1977) a bench top research device (Jones 1980b). A set of 9 permanent ring magnets ($B \approx 1{\cdot}5$ k Gauss) establish a picket fence confinement volume bounded by auxiliary toroidal and spindle cusps (figure 10). Modified hollow cathode discharges are used for plasma injection into the auxiliary cusps and serve to electrostatically plug the main confinement volume (Jones 1981). (Hollow cathodes are suitable for the present small scale experiment. For larger diameter injectors, however, one would have to use " plasma curtain " techniques which are not restricted to the small diameters of hollow cathode technologies, Jones 1980b, page 300). With another picket fence layer a thermal barrier could be built up.

Diagnostics consist of a set of Langmuir probes (which can be used) in the triple probe configuration (Chen and Sekiguchi 1965) and a high resolution planar gridded

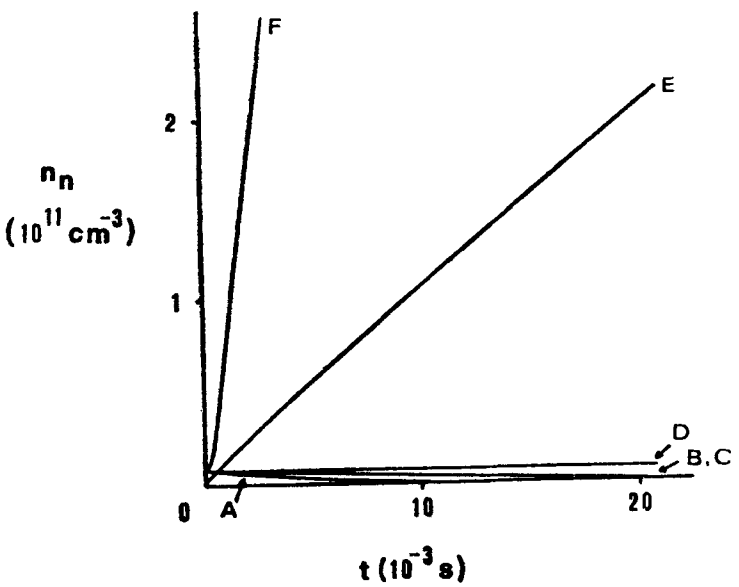


**Figure 9.** Neutral gas density *versus* time for various neutral models.

retarding field electrostatic energy analyzer (Jones 1978b). A pair of (internal and external) filaments are mounted on each hollow cathode (Jones 1980b) to improve the discharge ignition characteristics (*e.g.* reduce the overvoltage requirement). A cracked radio valve is used as a fast vacuum gauge probe (Inoue 1965–66).

## 6. Conclusions

Typical temporal evolution of the plasma parameters (in hydrogen for the given discharge power input measured across the device power supplies) is shown in figures 11 and 12 and the following conclusions are drawn.

(i) The neutral equation $n_e n_n$ = constant is a very poor model for the present experiment. Not only does the electron temperature experience an overshoot but the neutral pressure does not drop.
(ii) The neutral equation $n_e n_n^{-1}$ = constant, and, to a lesser degree $n_e n_n^{-1} = v_n (C_1 T_e + C_2 T_i)^{-1/2}$ predict an excessive neutral pressure increase.

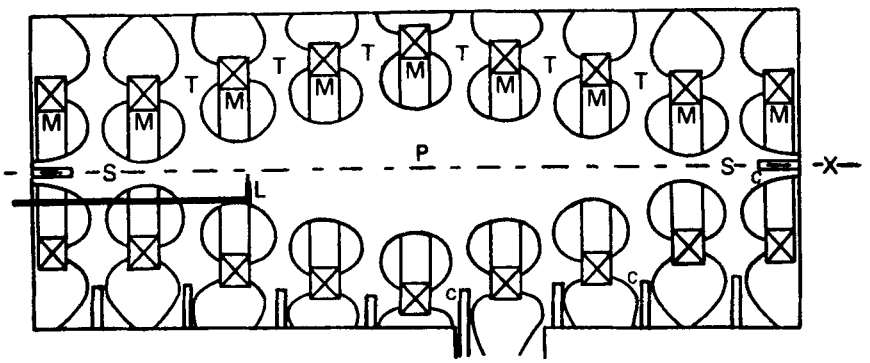


**Figure 10.** Experimental device having confined plasma region *P*, plugged by 6 toroidal cusp plasmas *T*, and 2 tandem spindle cusp plasmas *S*. Permanent ring magnets are marked *M* and typical hollow cathodes and probes marked C and L, respectively. Axis of cylindrical symmetry is marked X.

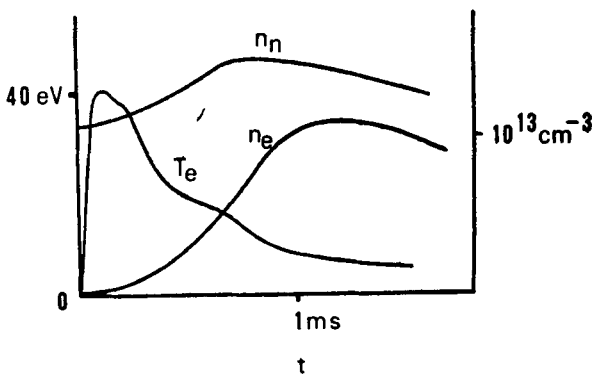


**Figure 11.** Temporal dependences of electron temperature $T_e$, plasma density, $n_e$, and neutral density $n_n$.

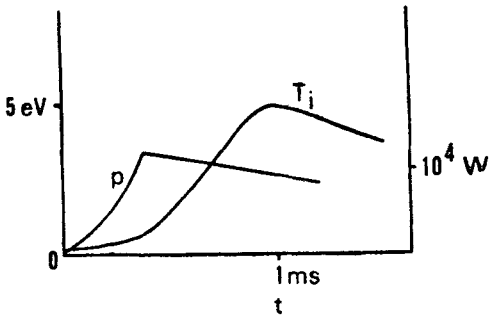


**Figure 12.** Temporal dependences of discharge power input $P$ and ion temperature $T_i$. Note: $P$ is not simply a constant.

(iii) The neutral equation $n_n$ = constant or $n_n v_n$ = constant has perhaps the best qualitative comparison with experiment but admixtures of several models cannot be ruled out.

Certainly all of the postulated models are oversimplifications. (The power input is time dependent, for instance, and $T_e$ may only approximate an anisotropic or runaway distribution early in time.) Although the experiment was not intended as a confinement study note the good energy confinement of the ES surface traps,

## Acknowledgements

The author would like to acknowledge the use of the Microcomputer Laboratory of the Physics Department, National University of Singapore and the assistance of Dr B Tan. This work was supported by grant N U S RP36/80. He also wishes to thank Prof. A Rajaratnam for his support and encouragement.

## References

Artsimovich L A 1972 *Nucl. Fusion* **12** 215
Berry L A, Clarke J F and Hogan J T 1974 *Phys. Rev. Lett.* **32** 362
Chen S L and Sekiguchi T 1965 *J. Appl. Phys.* **36** 2363
Cohen S A, Dylla H F, Rossnagel S M, Picraux S T, Borders J A and Magee C W 1978 *J. Nucl. Mater.* **76** 459
Drawin H W 1967 Euratom Report EUR-CEA-383, Fontenay-Aux-Roses, France
Goel N S, Maitra S C and Montrell E W 1971 *Rev. Mod. Phys.* **43** 231
Inoue N 1965-1966 *I P P Ann. Rev. Nagoya Univ. Jpn.* **24**
Jaegar E F and Hedrick C L 1979 *Nucl. Fusion* **19** 443
Jaeger E F, Hedrick C L and Ard W B 1979 *Phys. Rev. Lett.* **43** 855
Jones R 1977 *Plasma Phys.* **19** 925
Jones R 1978a *Phys. Lett.* **A67** 194
Jones R 1978b *Rev. Sci. Instrum.* **49** 21
Jones R 1979 *Pramāṇa* **12** 1
Jones R 1980a *IEEE Trans. Plasma Sci.* **8** 14
Jones R 1980b *Phys. Rep.* **61** 295, 300
Jones R 1980c *Pramāṇa* **15** 137
Jones R 1981 *Plasma Phys.* **23** 31

Kovrizhnykh L 1969 *JETP* **29** 475
Marmer E 1978 *J. Nucl. Mater.* **76** 59
McBride J B and Sultan A L 1978 *Nucl. Fusion* **18** 285
McCracken G M, Fielding S J, Erents S K, Pospieszczyk A and Stott P E 1978 *Nucl. Fusion.* **18** 35
Roth J R 1967 *Phys. Fluids* **9** 2713
Simonev V A, Shuilkin B N and Kutukov G P 1961 *Proc. IAEC Conf. on Plasma Phys. and Cont. Fusion* Salzburg
Sprott J C and Strait E J 1976 *IEEE Trans. Plasma Sci.* **4** 6